Dependence of Melt Behavior of Star Polystyrene/POSS Composites on the Molecular Weight of Arm Chains

ARTICLE *in* THE JOURNAL OF PHYSICAL CHEMISTRY B · APRIL 2014

Impact Factor: 3.3 · DOI: 10.1021/jp502946d · Source: PubMed

6 AUTHORS, INCLUDING:

Haiying Tan
Chinese Academy of Sciences
17 PUBLICATIONS **62** CITATIONS
SEE PROFILE

Donghua Xu
Changchun Insititue of Applied Chemistry, Chi…
38 PUBLICATIONS **1,187** CITATIONS
SEE PROFILE

THE JOURNAL OF PHYSICAL CHEMISTRY B

Article

pubs.acs.org/JPCB

Dependence of Melt Behavior of Star Polystyrene/POSS Composites on the Molecular Weight of Arm Chains

Haiying Tan,[†,‡] Jun Zheng,[†,‡] Donghua Xu,[†] Dong Wan,[†] Jian Qiu,[†] and Tao Tang*[,†]

[†]State Key Laboratory of Polymer Physics and Chemistry, Changchun Institute of Applied Chemistry, Chinese Academy of Sciences, Changchun 130022, China

[‡]Graduate School of the Chinese Academy of Sciences, Beijing 100039, China

Supporting Information

ABSTRACT: Rheological behavior of three-arm and six-arm star polystyrene (SPS) with a small amount of polyhedral oligosilsesquioxane (POSS) was studied. Both linear oscillatory frequency sweep and steady state shear results of SPS/POSS composites showed the reduction of melt viscosity in the unentangled SPS matrix and the increase of viscosity in the entangled SPS matrix. In particular, when molecular weight of the arm (M_a) of SPS was smaller than the critical molecular weight for entanglement (M_c) of PS, the melt viscosity of SPS/POSS composites with low content of POSS was lower than that of pure SPS. The abnormal phenomenon of reduced melt viscosity in SPS/POSS composites was in coincidence with the melt viscosity behavior of SPS/C_{60} composites reported in our previous work (*Soft Matter* **2013**, *9*, 6282−6290), although the diameters of two nanoparticles and their interaction with SPS matrix were different. A possible mechanism behind the melt viscosity behavior was discussed. Furthermore, the time−temperature superposition principle (TTS) was applied in SPS and SPS/POSS composites. The Cox−Merz empirical relationship was verified to be valid for SPS/POSS composites when the content of POSS was low (1 wt %).

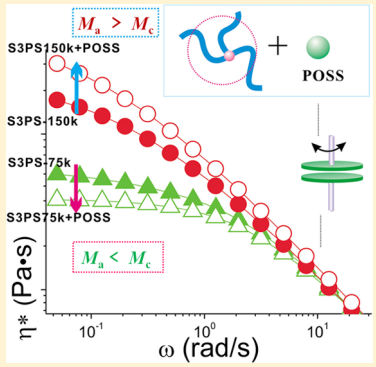

INTRODUCTION

Polymer nanocomposites fabricated by dispersing nanofillers in polymer matrices have the potential for enhancing performance that far exceeds traditional composites. The nanofillers may have spherical (C_{60}, etc.), layered (clay, graphene, etc.) or fibrous (carbon nanotubes, etc.) shapes. Polyhedral oligosilsesquioxane (POSS) is a class of organosilicic three-dimensional compounds with cage frameworks with different degrees of symmetry, and their general formula is $(RSiO1.5)n$, where n is an integer number and R is an organic group. POSS can be effectively incorporated into polymers by copolymerization,[1−4] grafting,[5] or even blending[6−9] (e.g., melt or solution mixing) via traditional processing methods. The incorporation of POSS and its derivatives into polymeric materials can lead to dramatic improvements in polymer properties, for example, increase in use temperature, surface hardening, oxidation resistance, and improved mechanical properties as well as reduction in flammability and melt viscosity during processing and so on.[2,10−12]

So far it is very interesting to understand the rheological behavior of polymers filled with nanoparticles, such as POSS. Wu et al.[13] studied the linear viscoelastic properties of entangled random copolymers from styrene and isobutyl POSS (iBuPOSS). The results revealed that the presence of iBuPOSS dramatically decreased the rubber plateau modulus, suggesting a strong dilation effect of iBuPOSS on entanglement density. Kopesky et al.[14] have also reported that tethered POSS incorporated within entangled poly(methyl methacrylate) (PMMA) leads to a decrease in the plateau modulus when compared to the case of the PMMA homopolymer. Romo-Uribe et al.[15] studied the viscoelastic properties of POSS−styrene macromolecules blended with polystyrene (PS). The presence of POSS−styrene macromolecules decreased the zero shear viscosity of the matrix, which might be attributed to the increase in the fractional free volume and reduction in the entanglement density.

The rheology of polymer/POSS composites, in which POSS and its derivatives were incorporated in polymer matrix by physically blending, was also studied. Fu et al.[16] studied the rheological behavior of POSS filled ethylene−propylene copolymer (EP). Oscillatory shear results showed that the EP/POSS nanocomposites exhibited a solid-like rheological behavior compared to the liquid-like rheological behavior in the neat resin. Joshi et al.[8] found that in the octamethyl POSS/high-density polyethylene (HDPE) nanocomposites, the presence of a small amount of POSS particles acted as lubricant and reduced the complex viscosity of the nanocomposites, but the viscosity increased at higher content. Morgan et al.[9] also found viscosity reduction in the nanocomposite (Tsp-POSS/PPSU) with only a small addition of POSS. This was attributed to internal lubrication resulting from the weak interfacial interactions between the components and the surface

Received: September 18, 2013
Revised: April 18, 2014
Published: April 23, 2014

   dx.doi.org/10.1021/jp502946d | *J. Phys. Chem. B* 2014, 118, 5229−5239

segregation of Tsp-POSS, which lubricated the exterior of the composite melt and reduced friction during processing.

Reviewing the previous reports, we found that the research was focused on the linear polymer/POSS composites. If polymer chains are long chain branched structure, such as star-like polymers or even comb-like polymers, how will their rheological behaviors change in the presence of POSS nanoparticles? In our previous work,[17] considering star-like polymer as the simplest long chain branched polymer, we have studied rheological behaviors of star polystyrene (SPS)/C_{60} composites and find that the incorporation of C_{60} into star polystyrene (SPS) decreases the melt viscosity of unentangled ($M_a < M_c$) SPS but increases the melt viscosity of the entangled SPS ($M_a > M_c$). A remaining question is whether the observed phenomenon in SPS/C_{60} composites is common in other long chain branched polymer/nanoparticles systems. In this work, the rheological behavior of SPS/POSS composites with low content of POSS was studied by linear oscillatory sweep and steady shear experiments. Although both C_{60} and POSS are nanosized particles, their sizes and interaction with SPS matrix may be different due to the different composition of the two nanoparticles. We want to know whether the phenomenon observed in SPS/C_{60} system also appears in SPS/POSS system.

EXPERIMENTAL SECTION

Materials. Octavinyl-polyhedral oligomeric silsesquioxane (POSS) was purchased from Hybrid Plastics Inc. Copper bromide (CuBr, 99.999%), 1,3,5-tribromomethylbenzene, and 1,2,3,4,5,6-hexakis(bromomethyl)benzene were purchased from Aldrich. 2,2′-Dipyridyl was purchased from TCI. Styrene (99%), toluene, tetrahyrofuran (THF), CH_2Cl_2, hexane, methanol, and neutral alumina were purchased from China National Medicines Corporation Ltd. Styrene was distilled over CaH_2 prior to use. Toluene was purified by the Braun system. All the other reagents were used as received. Synthesis of star polystyrene (SPS) was reported elsewhere,[17] and the molecular weight and radius gyration of the synthesized SPS are shown in Table 1. The SPS was nominated as S*x*PS-*y*, here "*x*" represented the arm number of SPS, and *y* represented molecular weight of SPS. For example, S3PS-75k meant three-arm star PS with the molecular weight of 75k.

Table 1. Structure Information of Three-Arm PS (S3PS) and Six-Arm PS (S6PS) from Triple Detection Size Exclusion Chromatography (SEC−MALS)

sample	M_w[a] (kDa)	PDI	M_a[b] (kDa)	R_g (nm)
S3PS-48k	48.2	1.13	16.0	5.3
S3PS-75k	74.9	1.13	25.0	8.7
S3PS-119k	118.9	1.30	39.6	11.1
S3PS-150k	150.0	1.66	50.0	13.5
S6PS-93k	93.0	1.16	15.5	6.8
S6PS-226k	226.3	1.18	37.7	10.8

[a]Molecular weight of the arm (M_a) of start PS was determined by the relationship $M_a = 1/3M_w$ in S3PS, $M_a = 1/6M_w$ in S6PS.

Sample Preparation. POSS was dissolved in toluene at a concentration of 2 mg/mL. Next, a certain amount of PS/toluene solution was added to POSS/toluene solution to obtain the desired weight fractions of POSS in the final composite. The mixed solutions were stirred and then added dropwise into a large volume of methanol to get coprecipitation of PS and POSS. The solids were filtered from methanol and dried under vacuum at 80 °C for more than 24 h to remove solvent. Before rheological testing, the samples were treated at 130−170 °C under vacuum for several hours to ensure homogeneity. The obtained composite samples were molded by compression into round pieces (25 mm diameter) under vacuum to ensure that no trapped air remained within the samples. All the samples for rheological testing were prepared under the same conditions.

Characterization. The dispersion state of the SPS/POSS nanocomposites was observed by transmission electron microscopes (TEM, JEOL1011 JEOL, Japan) and a high resolution transmission electron microscope (Tecnai G2 F20 FE-TEM, FEI, Holland) on microtome sections at 100 and 200 kV accelerating voltage, respectively. Ultrathin sections of the sample, which had been pressed into a sheet, were cut on a Reica Ultracut microtome equipped with a glass knife at room temperature. The samples were collected on carbon-coated copper TEM grids.

The glass transition temperature (T_g) of samples was measured by differential scanning calorimetry (DSC, Mettler Toledo DSC 1, Switzerland). Samples of about 10 mg were loaded in aluminum pans and heated at a rate of 10 °C/min under a nitrogen atmosphere. A first scanning was carried out from ambient temperature to 200 °C, and the samples were held for 3 min in the molten state to erase previous unknown thermal history. Then the samples were cooled to 20 °C and a second heating scan was carried out with heating to 200 °C. The temperature corresponding to the midpoint in the heat capacity step-rise was used for the determination of T_g.

The rheological properties of samples were performed on a strain-controlled rheometer (ARES-G2, TA Instruments) using a plate−plate geometry (25 mm diameter). The temperature was controlled by a forced convection oven (FCO) unit under a nitrogen gas purge to minimize the degradation of the samples. A strain amplitude sweep (0.01−100%) at a fixed frequency (ω = 1 rad/s) was performed to establish the linear viscoelastic regime. Frequency sweeps in the range 0.1−100 rad/s were performed at various temperatures. These were then combined using time−temperature superposition to yield a master curve at 150 °C. A dwell time of 5 min was allowed at each temperature for the samples to attain a uniform melt temperature, before commencing measurements. Flow sweeps were performed from 10^{-4} to 10 s^{-1}. The experimental temperature was 150 °C without other notes.

RESULTS AND DISCUSSION

Linear Oscillatory Frequency Sweep. The melt viscosity behavior of SPS/POSS composites was first studied by linear oscillatory frequency sweep experiments. Figure 1 shows complex viscosity (η^*) versus angular frequency (ω) for

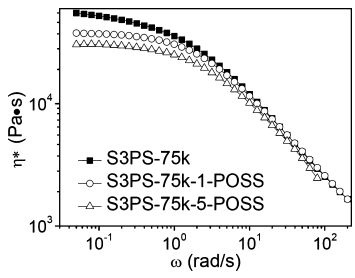

Figure 1. Complex viscosity (η^*) vs angular frequency (ω) for S3PS-75k with POSS in the concentrations of 1 and 5 wt % at 150 °C.

dx.doi.org/10.1021/jp502946d | J. Phys. Chem. B 2014, 118, 5229−5239

S3PS-75k/POSS composites. The η^* of S3PS-75k/POSS composites with 1 wt % POSS was lower than that of pure S3PS-75k. When the content of POSS was increased to 5 wt %, the η^* of S3PS-75k/POSS composites further decreased. The changing trends of storage (G') and loss (G'') moduli for S3PS-75k with POSS were similar to that of the η^* (Figure S1 in Supporting Information). For S3PS-48k, the addition of 1 wt % POSS also resulted in the reduced melt viscosity, which is similar to that of S3PS-75k/POSS (Figure S2 in Supporting Information). From the above results, when the molecular weight of the arm (M_a) of S3PS is smaller than the critical entanglement molecular weight (M_c), the M_c for the PS melt was ~33 kDa at 150 °C),[18,19] the η^* of S3PS/POSS composites with low concentration of POSS is lower than that of pure S3PS matrix.

Figure 2 shows the η^* plots versus the ω for S3PS-150k ($M_a > M_c$) and its composites with POSS. The η^* of S3PS-150k/

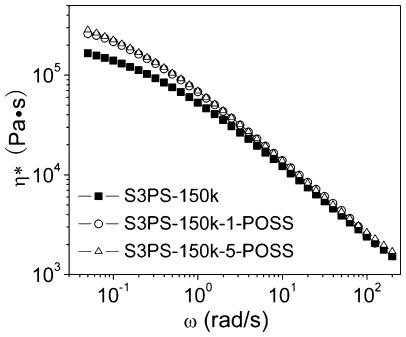

Figure 2. Complex viscosity (η^*) vs angular frequency (ω) for S3PS-150k samples with POSS in the concentrations of 1 and 5 wt % at 150 °C.

POSS composites was always higher than that of the pure S3PS-150k matrix, which is similar to the results in S3PS-150k/C_{60} composites.[17] The changing trends of G' and G'' in S3PS-150k/POSS composites are also similar to that of the η^* in Figure 2 (Figure S3 in Supporting Information). For S3PS-119k, the addition of POSS also increased the melt viscosity S3PS-119k (Figure S4 in Supporting Information). In a word, the η^* POSS/S3PS composites is higher than that of pure S3PS matrix, when the M_a of S3PS is larger than the M_c of PS.

We further explored the melt viscosity behavior of SPS/POSS composites, where the arm number of SPS was six (S6PS). The η^* of S6PS-93k composites with 1 wt % POSS was lower than that of the pure S6PS-93k matrix (Figure 3a). This is consistent with the melt viscosity behavior of S3PS/POSS composites where the M_a of S3PS is smaller than the M_c of PS (Figure 1). When the content of POSS increased to 5 wt %, the melt viscosity of S6PS-93k-5-POSS was higher than that of S6PS-93k-1-POSS but still lower than that of S6PS-93k. Compared to η^* of S6PS-226k, the increment in the η^* (at low shear frequencies) of S6PS-226k composites with 1 wt % POSS at 150 °C was subtle (Figure 3b), which is ascribed to the lower testing temperature. When the testing temperature was increased to 170 °C, the differences in η^* were clearly observed (see inset in Figure 3b). When the content of POSS increased to 5 wt %, the melt viscosity was further increased. It could be seen that the changing trend in the melt viscosity of S6PS-226k/POSS composites was similar to that of S3PS-150k composites (Figure 2) where the M_a of SPS was higher than the M_c of PS. The changing trends of G' and G'' of S6PS-93k and

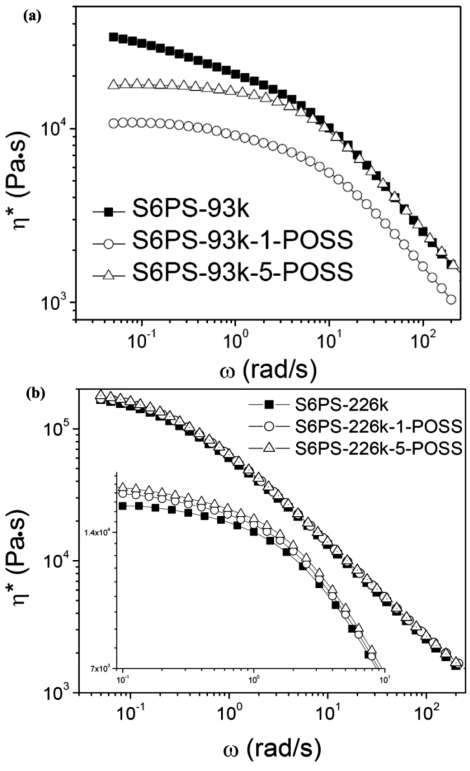

Figure 3. Complex viscosity (η^*) vs frequency (ω) for (a) S6PS-93k and (b) S6PS-226k with POSS in the concentrations of 1 and 5 wt % at 150 °C. Inset: complex viscosity (η^*) vs frequency (ω) for S6PS-226k at 170 °C.

S6PS-226k with POSS are also similar to that of the η^* in Figure 3 (Figure S5 and Figure S6 in Supporting Information). These results suggest that the melt viscosity of S6PS/POSS composites shows a similar melt behavior with that of S3PS/POSS composites although the arm number in both star-like PS matrices is different.

According to the results from linear oscillatory frequency sweep, the plateaus modulus (G_N^0) of the sample can be obtained by the "MIN method":[20]

$$G_N^0 = G'(\omega)_{\tan\delta\to\min} \quad (1)$$

where tan δ is the damping factor, and the value of G' at the minimum of tan δ is G_N^0.

The apparent relaxation time (τ_a) of a sample was calculated from the crossover frequency (ω_c) of G' and G'' from the linear frequency sweep results ($\tau_a = 1/\omega_c$).[21] Table 2 summarizes various rheological parameters and glass transition temperature (T_g) of the samples. When the M_a of SPS was smaller than the M_c of PS, the incorporation of POSS decreased the τ_a. In contrast, when $M_a > M_c$, the τ_a increased after the addition of POSS. Thus, the relaxation time showed a similar changing trend to the viscosity in the studied system. However, the changing trend of G_N^0 with the addition of POSS was complicated (Table 2). There was no close relation between viscosity change and G_N^0.

Time−Temperature Superposition. The dynamic moduli within the linear viscoelastic regime were characterized by frequency sweep in a range of temperatures from 150 to 210 °C. All of the experiments were within the linear viscoelastic regime determined by strain sweep tests. Relative to a fixed reference temperature (T = 150 °C), we applied the time−

dx.doi.org/10.1021/jp502946d | J. Phys. Chem. B 2014, 118, 5229−5239

Table 2. Cross Frequency (ω_{cross}), Apparent Relaxation Time (τ_a), Plateau Modulus (G_N^0), Apparent Viscosity (η_a), Zero Shear Viscosity (η_0), and Glass Transition Temperature (T_g) for Pure SPS and Their Composites with POSS at 150 °C

sample	ω_{cross} [a] (rad/s)	G_N^0 (MPa)	τ_a (s)	η_a [b] (Pa · s)	η_0 [c] (Pa · s)	T_g (°C)
S3PS-75k-0	4.134	0.171	0.242	41374	55859	104.1
S3PS-75k-1-POSS	5.785	0.184	0.173	31906	41448	103.7
S3PS-75k-5-POSS	7.175	0.156	0.139	21771	40825	104.6
S3PS-150k-0	0.802	0.148	1.248	185031	189011	105.8
S3PS-150k-1-POSS	0.296	0.132	3.381	447514	442895	104.3
S3PS-150k-5-POSS	0.278	0.127	3.590	456150	452690	105.1
S6PS-93k-0	14.193	0.209	0.070	14764	40644	102.7
S6PS-93k-1-POSS	27.106	0.154	0.037	5692	21998	101.0
S6PS-93k-5-POSS	20.811	0.197	0.048	9456	20104	103.4
S6PS-226k-0	0.748	0.157	1.338	210338	182754	104.3
S6PS-226k-1-POSS	0.723	0.142	1.384	197568	229743	103.3
S6PS-226k-5-POSS	0.712	0.139	1.404	195224	212700	104.7

[a]Angular frequency where the storage modulus equals the loss modulus. [b]Apparent viscosity determined from the relationship: $\eta_a = \tau G_N^0$. [c]Zero shear viscosity determined from the plateau region of steady state shear viscosity.

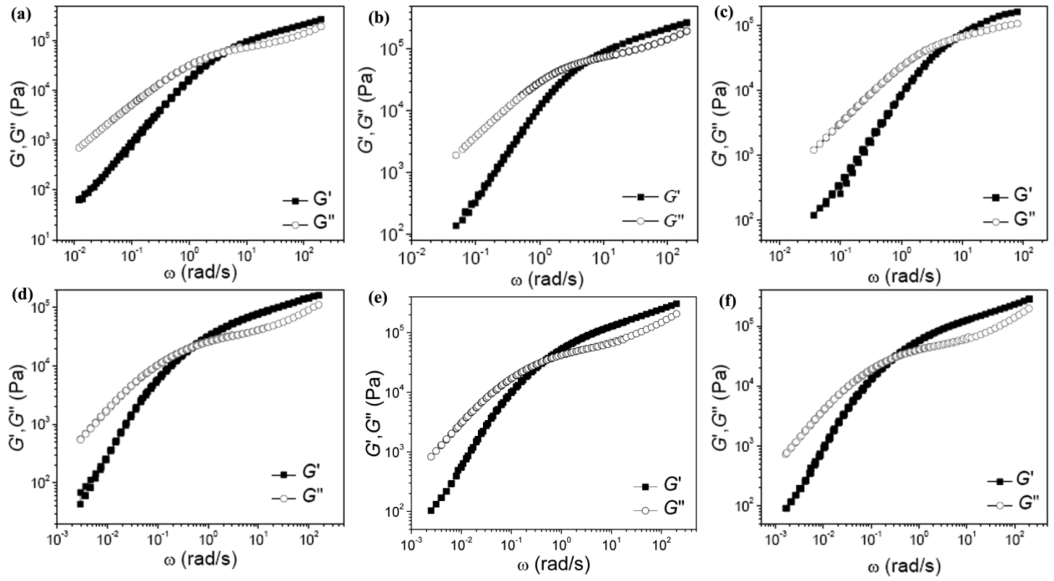

Figure 4. Master curves of dynamic moduli (square symbols for $G'(\omega)$ and circle symbols for $G''(\omega)$) vs angular frequency (ω) for (a) S3PS-75k, (b) S3PS-75k-1-POSS, (c) S3PS-75k-5-POSS, (d) S3PS-150k, (e) S3PS-150k-1-POSS, and (f) S3PS-150k-5-POSS (T_{ref} = 150 °C).

temperature superposition (TTS) principle:[22] by shifting the logarithmic plots of $G'(\omega)$ and $G''(\omega)$ along the frequency axis (horizontally). Vertical shifts along the modulus axis were not required. Thus, for good superposition:

$$G^{\#}(\omega,T) = G^{\#}(\omega,\alpha_T,T_{ref}) \quad (2)$$

where the symbol (#) stands for either one prime (′) or two primes (″), T_{ref} is the reference temperature, and α_T is the temperature dependent frequency shift factor. Figure 4 shows the master curves of the pure polymeric components and their composites with POSS. Parts a and d of Figure 4 show the master curves for the $G'(\omega)$ and $G''(\omega)$ as a function of ω for the neat S3PS-75k and S3PS-150k, respectively. The pure S3PS showed a predominantly viscous behavior ($G''(\omega) > G'(\omega)$) at low frequencies and a transition toward the rubberlike regime ($G'(\omega) > G''(\omega)$) at intermediate frequencies. Within the testing temperature range, the TTS principle was applicable. Parts b, c, e, and f of Figure 4 show the master curves for S3PS-75k-1-POSS, S3PS-75k-5-POSS, S3PS-150k-1-POSS, and S3PS-150k-5-POSS composites, respectively. The composites showed a similar rheological behavior to that displayed by S3PS matrix, and the TTS principle was found to be satisfactory and applicable within the temperature range investigated.

The $\alpha_T(T)$ can be described by the WLF equation,[22] which is derived on the basis of temperature dependent free volume:

$$\log \alpha_T = -C_1^g(T - T_g)/(C_2^g + (T - T_g)) \quad (3)$$

here, $C_1^g = B/2.303\, f_g$ and $C_2^g = f_g/\alpha_f$, where f_g is the fractional free volume at T_g, α_f is the temperature coefficient of fractional free volume, and B is a constant, generally assumed to be unity. If the reference temperature, T_{ref}, is different from the T_g, the WLF equation will be rewritten as

$$\log \alpha_T = -C_1^{ref}(T - T_{ref})/(C_2^{ref} + (T - T_{ref})) \quad (4)$$

where $C_1^{ref} = B/2.303\, f_{ref}$, $C_2^{ref} = f_{ref}/\alpha_f$, and f_{ref} is the fractional free volume at the T_{ref}.

Inspection of eq 4 reveals that the plot of $1/\log(\alpha_T)$ vs $1/(T - T_{ref})$ should be linear (if the expression holds) and that the parameters (C_1^{ref} and C_2^{ref}) may be determined from the slopes and intercepts of the plots. For all the composites examined, such plots (Figure 5) indeed show a linear relationship,

dx.doi.org/10.1021/jp502946d | J. Phys. Chem. B 2014, 118, 5229−5239

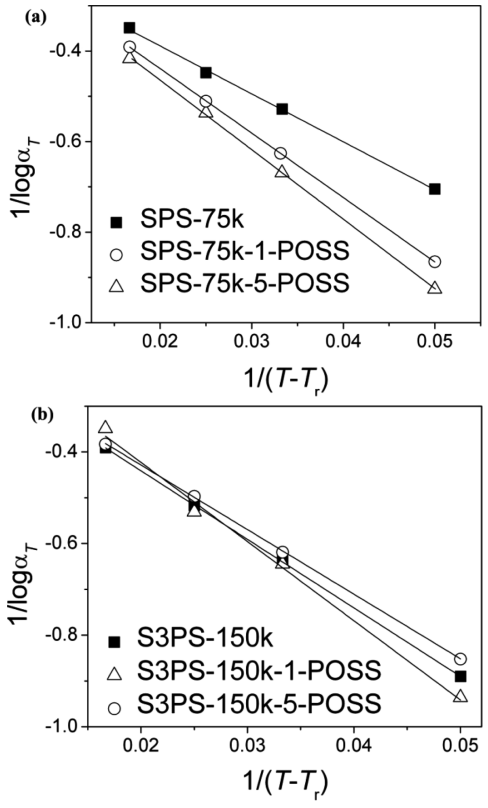

Figure 5. WLF function plots of shift factor (α_T): (a) S3PS-75k (square) and its composites (circle for S3PS-75k-1-POSS and triangle for S3PS-75k-5-POSS); (b) S3PS-150k (square) and its composites (circle for S3PS-150k-1-POSS and triangle for S3PS-150k-5-POSS).

indicating the validity of eq 4. From the slopes and intercepts, C_1^{ref}, C_2^{ref}, f_{ref}, and α_f for each sample are determined, whose values at the T_g can be calculated using the following equations:[22]

$$C_1^g = C_1^{ref} C_2^{ref} / (C_2^{ref} + T_g - T_{ref}) \quad (5)$$

$$C_2^g = C_2^{ref} + T_g - T_{ref} \quad (6)$$

$$f_g = B(C_2^{ref} + T_g - T_{ref}) / (2.303 C_1^{ref} C_2^{ref}) \quad (7)$$

The calculated values of the free volume parameters for the S3PS/POSS composites are listed in Table 3. The results showed that the fractional free volume (f_{ref}) at the reference temperature (150 °C) decreased after the addition of POSS in S3PS-75k ($M_a < M_c$). However, the fractional free volume (f_g) at T_g increased on the addition of POSS. Meanwhile, fitting to the experimental data showed that the thermal expansivity (α_f) decreased with the addition of POSS (Table 3). For S3PS-150k, the addition of POSS also decreased the f_{ref} and α_f but increased the f_g.

Table 3. Viscoelastic Properties of S3PS-75k, S3PS-150k, and Their Composites at T_{ref} = 150 °C[a]

sample	C_1^{ref}	C_2^{ref}	f_{ref}/B	α_f/B ($\times 10^{-4}$)	f_g/B
S3PS-75k-0	5.90	64.16	0.0736	11.47	0.0211
S3PS-75k-1-POSS	6.54	93.56	0.0664	7.10	0.0335
S3PS-75k-5-POSS	6.04	90.79	0.0719	7.92	0.0359
S3PS-150k-0	6.02	81.75	0.0721	8.82	0.0331
S3PS-150k-1-POSS	7.31	115.58	0.0594	5.14	0.0359
S3PS-150k-5-POSS	7.53	114.06	0.0577	5.08	0.0349

[a]All the data were determined from the relationship as described in the text.

According to the WLF theory[23] (shown in Figure 5), the fractional free volume f can be written approximately as $f = f_g + \alpha_f(T - T_g)$ for $T > T_g$. Applying this relation and using the experimentally determined values for all the parameters, the temperature dependence of the free volume fraction for S3PS and S3PS/POSS composites within the temperature range 150 °C < T < 210 °C can be obtained (Figure 6). The free volume

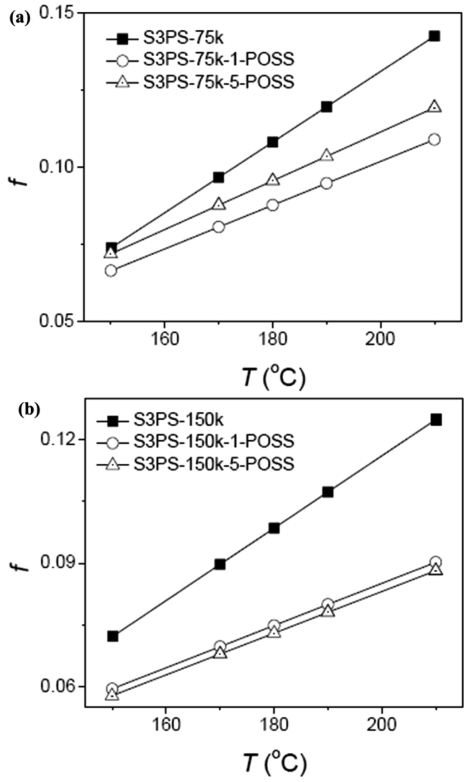

Figure 6. Temperature dependence of fractional free volume (f) for (a) S3PS-75k and its composites (S3PS-75k (square), S3PS-75k-1-POSS (circle), and S3PS-75k-5-POSS (triangle)) and (b) for S3PS-150k and its composites (S3PS-150k (square), S3PS-150k-1-POSS (circle), and S3PS-150k-5-POSS (triangle)).

of the polymer matrix increased with the temperature. The incorporation of nanoparticles (POSS) decreased the free volume of both entangled and unentangled S3PS/POSS composites compared to that of the pure polymer matrix.

Steady Shear Results. Figure 7 shows the plots of steady shear viscosity as a function of shear rate for the pure SPS and the composites. The shear viscosity of unentangled S3PS-75k and S6PS-93k decreased substantially with the incorporation of POSS. Furthermore, like a typical polymer, SPS and their composites exhibit a Newtonian plateau region at low shear rate. The zero shear viscosity (η_0) can be directly obtained from the plateau at extremely low shear rates as shown in Figure 7. The addition of POSS caused the reduction in melt viscosities, which are coincidence with the linear oscillatory frequency sweep results.

Figure 8 shows the changing trends in steady state shear viscosity of entangled ($M_a > M_c$) SPS on the addition of

dx.doi.org/10.1021/jp502946d | J. Phys. Chem. B 2014, 118, 5229−5239

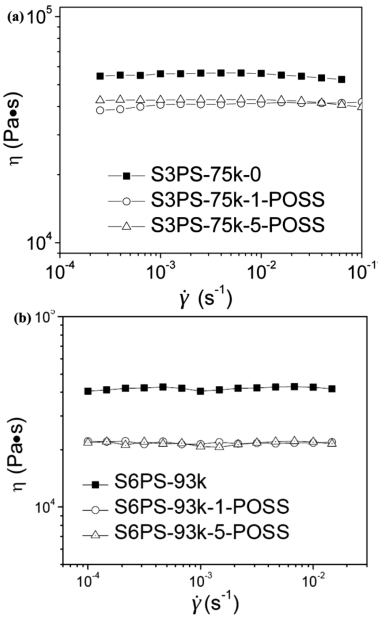

Figure 7. Steady state shear viscosity as a function of shear rate for S3PS-75k and S6PS-93k and their composites with 1 and 5 wt % of POSS at 150 °C.

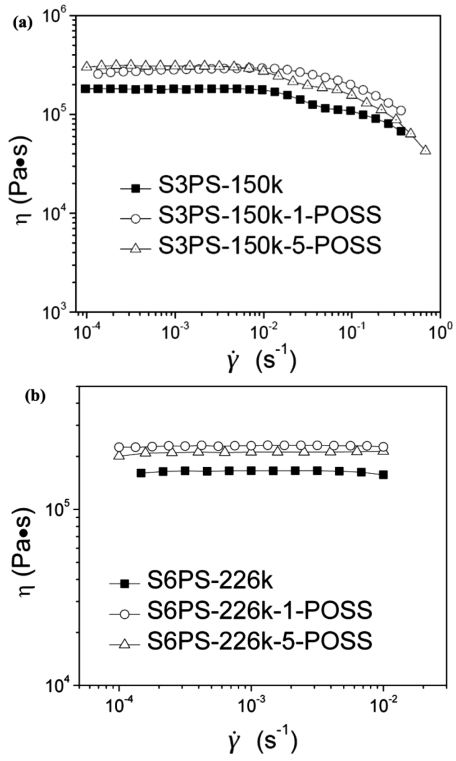

Figure 8. Steady state shear viscosity as a function of shear rate for S3PS-150k and S6PS-226k and their composites with 1 and 5 wt % POSS at 150 °C.

nanoparticles, demonstrating that the addition of POSS increased the shear viscosity of S3PS-150k and S6PS-226k, respectively. The results are also in accordance with those from linear oscillatory frequency sweep. The shear viscosities versus shear rates of S3PS-48k, S3PS-119k, and their composites with 1 wt % POSS are shown in Figure S7 (Supporting Information).

The so-called Cox–Merz "rule",[24] an empirical relationship that has been found to be of great use in rheology, was checked in this work. It was observed by Cox and Merz that for many polymeric systems the correlation occurred between the steady state shear viscosity (η) plotted against shear rate (γ) and the magnitude of the complex viscosity (η^*) plotted against angular frequency (ω). The complex viscosity is defined by $\eta^* = G^*/i\omega$, where G^* is the complex modulus. The dynamic viscosity and the steady state viscosity are equal in the low frequency and shear rate limits, i.e.:

$$\eta'(\omega)|_{\omega\to 0} = \eta(\gamma)|_{\gamma\to 0} \quad (8)$$

The elastic contribution to $\eta'(\omega)$ disappears in the low frequency limit, and eq 8 can be rewritten as

$$\eta^*(\omega)|_{\omega\to 0} = \eta(\gamma)|_{\gamma\to 0} \quad (9)$$

Milner[25] has used the Doi–Edwards reptation model[26] to provide a theoretical basis for the rule. Figure 9 shows that the

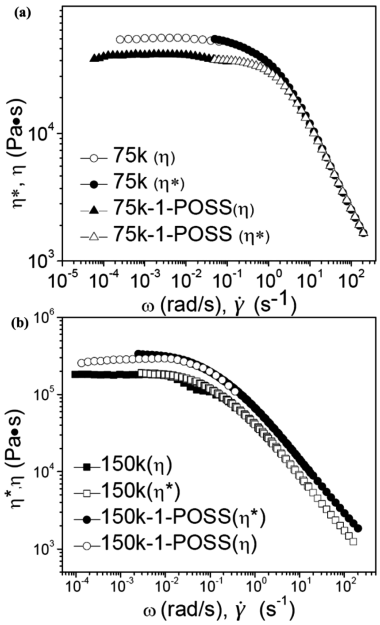

Figure 9. Dynamic and steady state viscosities plotted on the same graph for S3PS-75k and S3PS-150k and their composites with 1 wt % of POSS at 150 °C.

Cox–Merz empirical relationship between the linear (oscillatory) and nonlinear (steady-shear) viscosity is valid for both the entangled and unentangled SPS system. Furthermore, the viscosity of the composites with the incorporation of 1 wt % POSS also follows the Cox–Merz rule. This means that the η_0 obtained from the complex viscosity at very low shear frequencies from linear oscillatory frequency sweep is equal to that from the steady state shear viscosity at very low shear rate. However, when the content of POSS in the SPS matrix increased to 5 wt %, Cox–Merz empirical relationship between the linear (oscillatory) and nonlinear (steady-shear) viscosity was failed (Figure S8, Supporting Information). This might be caused by the formation of large aggregates (Figure S9, Supporting Information) in the SPS matrix at the content of 5 wt % POSS.

Relaxation Spectrum. As mentioned-above, the rheological properties of samples are related to their relaxation mode. Figure 10 shows the continuous relaxation spectra of SPS-75k,

dx.doi.org/10.1021/jp502946d | J. Phys. Chem. B 2014, 118, 5229–5239

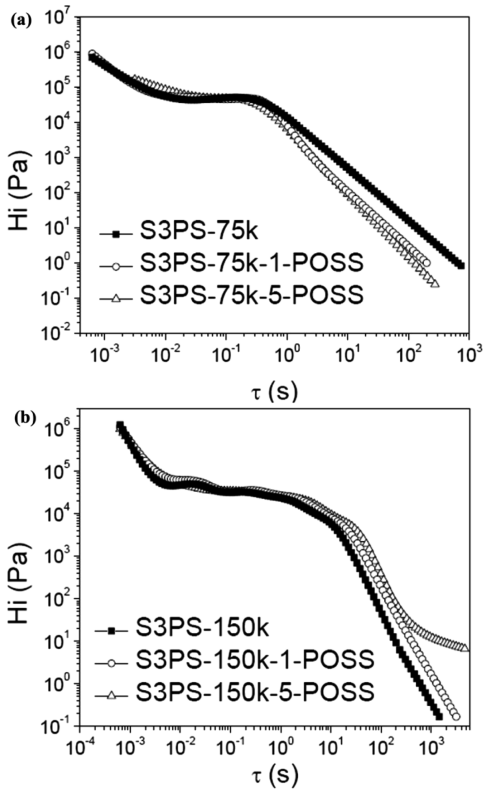

Figure 10. Relaxation spectra for pure S3PS-75k, S3PS-150k, and their composites with POSS: (a) S3PS-75k; (b) S3PS-150k.

SPS-150k, and their composites, calculated from frequency sweep at 150 °C. At short time scale, the presence of POSS did not significantly affect the Rouse or the plateau regime of the relaxation spectra of S3PS-75k or S3PS-150k. Instead, at longer time scale, the presence of POSS influenced the terminal region of the relaxation spectra of SPS composites. Compared to the relaxation behavior of pure S3PS-75k matrix, the apparent reduction of the longest relaxation times of S3PS-75k with 1 and 5 wt % POSS was observed (Figure 10a). In contrast, the longest relaxation times of S3PS-150k/POSS composites were longer than that of pure S3PS-150k matrix (Figure 10b). All the data from the entangled and unentangled systems show that the presence of a small amount of nanoparticle strongly influences the long relaxation model. These are consistent with the changing trends of η_0 (Table 2).

Discussion. So far the reduced melt viscosity of polymer composites after the incorporation of isotropic nanoparticles has been just reported in linear entangled polymer systems, such as C_{60} or Fe_3O_4 in PS,[27] polysilicates in PDMS,[28,29] POSS in PS or HDPE,[8] $CaCO_3$ in polypropylene,[30] etc. On summarizing these reports,[18,27−29] in linear polymer systems, there are three preconditions to be satisfied: (i) the diameter of particles (R_p) being smaller than the gyration radius (R_g) for the polymer, (ii) the polymer being above the entanglement molecular weight, and (iii) the average interparticle half-gap (h) being smaller than the R_g of polymer. Very recently, we have found that the presence of the well-dispersed C_{60} reduces the viscosity of unentangled star PS (SPS) melts ($M_a < M_c$) but increases the viscosity of entangled SPS ($M_a > M_c$).[17] In this work, we find a similar phenomenon on the changing trend of melt viscosity of SPS when POSS is used to replace C_{60} in the SPS matrix; that is, the addition of a small amount of POSS decreases the complex viscosity of unentangled SPS and increases the complex viscosity of entangled SPS. It is clear that the appearance of reduced viscosity in polymer/nanoparticles systems with a small amount of nanoparticles strongly depends on the molecular weight of linear polymers or the arm molecular weight of star polymers. The diameters of C_{60} and POSS are 0.7[27] and 1.5 nm,[13] respectively, which are smaller than the R_g of SPS. The ratio of the average interparticle half-gap (h) to the R_g of polymer is also an important factor to influence the viscosity changing trend of linear polymer after adding some nanoparticles. The h can be calculated from the following relationship:[27]

$$h/R = [\phi_m/\phi]^{1/3} - 1 \tag{10}$$

where ϕ_m is the maximum random packing volume fraction (~0.638) and ϕ is the volume fraction of nanoparticle. In the SPS composites with 1 wt % POSS or C_{60}, the h is about 1.3 and 2.8 nm, respectively. The h will decrease when the content of nanoparticles increases. Thus, it can be seen that the h is smaller than the R_g of SPS in the SPS/C_{60} and SPS/POSS composites, despite the arm molecular weight of SPS.

Another important factor is the interaction between polymer chains and nanoparticles, which determines the dispersed states of nanoparticles in polymer matrix, although the preparation methods for polymer composites may influence the dispersed states of nanoparticles.[27] According to the reported method for estimating Flory−Huggins interaction parameters (χ), the χ between polymer and nanoparticle can be estimated from the Hildebrand solubility parameters:[31,32]

$$\chi = \frac{\nu_{seg}}{RT}(\delta_1 - \delta_2)^2 \tag{11}$$

where ν_{seg} is the actual volume of a polymer segment, R is the ideal gas constant, T is the absolute temperature, and δ_1 and δ_2 are the solubility parameters of polymers and nanoparticles, respectively. The χ between PS and C_{60} is 0.015,[32] which indicates a stronger attractive interaction between C_{60} and PS. According to the solubility parameters of PS (19.35 (cal/cm^3)$^{1/2}$) and POSS with octavinyl vertex groups (16.05 (cal/cm^3)$^{1/2}$) reported by Dintcheva,[33] the calculated χ between PS and POSS is 0.061, indicating a weak attractive interaction between POSS and PS compared to that between C_{60} and PS. The weak attractive interaction should result from the contribution of the dispersion forces between vinyl groups linked to the vertex of POSS and PS. Because organic groups linked to the vertex of POSS are able to exert a shielding effect of the POSS inorganic framework, the interaction between the matrix macromolecules and the POSS inorganic core is much less pronounced.

The morphologies of SPS/POSS composites were explored by TEM. The dispersion states of POSS (1 and 5 wt %) in S3PS-75k and S3PS-150k are shown as examples (Figure S9, Supporting Information). POSS was well dispersed in the S3PS-75k matrix. Also most of POSS was well dispersed in S3PS-150k matrix, but some aggregates of POSS could be found. When the content of POSS increased to 5 wt %, larger aggregates were formed. Comparing the results in Figure 1 and Figure 3a with the TEM results in Figure S9 (Supporting Information), the presence of POSS (1 and 5 wt %) in unentangled SPS matrices led to the reduced viscosity although the dispersion states of POSS was different. This implies that the different melt viscosity behavior of unentangled ($M_a < M_c$)

dx.doi.org/10.1021/jp502946d | J. Phys. Chem. B 2014, 118, 5229−5239

and entangled ($M_a > M_c$) SPS after the incorporation of POSS cannot be ascribed to the dispersion states of POSS in SPS matrices.

Although the size of nanoparticles (POSS or C_{60}) and the interaction between SPS and nanoparticles (POSS or C_{60}) are different in SPS/POSS and SPS/C_{60} composites, the addition of POSS or C_{60} into the SPS matrix shows a similar changing trend in the melt viscosity compared to that of pure SPS. It is an interesting issue why the molecular weight of the arm chains in the SPS shows a strong influence on the melt viscosity behavior of SPS/POSS (or C_{60}) composites when the content of these nanoparticles is low. The concept of excluded free-volume induced around the nanoparticles was used by Mackay et al. to explain the decrease in the viscosity of linear polymer/nanoparticle melts.[15] In this work, the rheological results show that the free volume at the measured temperature decreases in both the entangled and unentangled SPS/POSS systems compared to the case of pure SPS (Table 3 and Figure 6), demonstrating that the space left for the movement of the chain become smaller, so the viscosity should increase. However, the case is contrary in the unentangled SPS system (Figures 1 and 3a). So the change of free volume is not the key factor that is responsible for the viscosity change of SPS/POSS composites.

When the data of η_0 and τ_a shown in Table 2 are compared, all the data from the entangled and unentangled systems show that the presence of POSS strongly influences the viscosity and relaxation time. Moreover, the viscosity changing trend is similar to the changing trend of relaxation time. As we know, the viscosity is a function of product of plateau modulus (G_N^0) and relaxation time. To clarify the relationship between η_0 and τ_a, here the apparent viscosity (η_a) is defined by the relationship: $\eta_a = G_N^0\tau$.[19] Generally speaking, the G_N^0 of SPS/POSS composite does not change monotonically with the incorporation of POSS (Table 2). Summarizing the data of η_a, the relaxation time, and G_N^0 in both the entangled and unentangled system, we see that the changing trend of η_a is not in accordance with that of plateau modulus in SPS/POSS composites, but in accordance with terminal relaxation time. From these results we conclude that the presence of POSS changes the relaxation mode of SPS chains. Further investigations, especially theoretical and simulation works, are needed to thoroughly understand the mechanism behind the melt viscosity behavior of star polymer/nanoparticle composites.

Here we propose a possible model (Figure 11), based on our experimental observations, to provide a microscopic understanding of the physics relating the dependence of melt behavior on the molecular weight of arm chains in star polymers after adding POSS (or C_{60}). It is clear that the dependence of melt viscosity behavior of star polymer/nanoparticle composites on the molecular weight is totally different from that of linear polymer/nanoparticle composites. The main difference between star polymer and linear polymer systems is the topological structure of polymer chains, which is the key factor determining the different changing trends in the melt viscosities of SPS/C_{60} and linear PS/C_{60} composites.[17] Why does the topological structure of polymer chains play a key role in the melt viscosity behavior of polymer/nanoparticle systems? In a linear polymer matrix, a nanoparticle, which has attractive interaction with polymer chains (otherwise the nanoparticles could not be well dispersed in polymer matrix to form polymer nanocomposites), can be freely dispersed in any region of polymer matrix (left picture in Figure 11). When

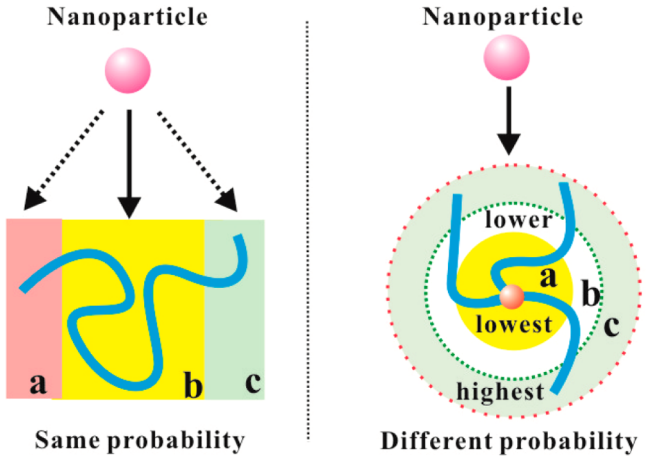

Figure 11. Schematic diagram of the possible distribution of nanoparticles in linear polymer (left) and star polymer (right).

the M_w is higher than M_c, the melt viscosity of linear polymer mainly depends on the number of chain entanglements. In this case, the addition of nanoparticles will reduce the number of chain entanglement.[28] As a result, the melt viscosity decreases compared to the melt viscosities of the parental linear polymers. However, there is also interaction between polymer chains and nanoparticles, which results in the increase of melt viscosity. When the interaction between polymer and nanoparticles is medium attractive, the melt viscosity of linear polymer/nanoparticle systems is lower than that of the parental linear polymer. Otherwise, the melt viscosity of linear polymer/nanoparticle systems may be higher than that of the parental linear polymer, if the interaction between polymer and nanoparticles is strong attractive.[34] When the M_w is lower than the M_c, there is no entanglement between polymer chains. In this case, the added nanoparticles have the interaction with polymer chains, which leads to the increase of melt viscosity of the nanocomposites compared to that of the pure linear polymer matrix.

In the star-like polymer/nanoparticle system, in which polymer matrix has attractive interaction with the nanoparticles, we have supposed that the nanoparticles could not be dispersed freely in any region of polymer matrix due to spatial limit of star topological structure (right picture in Figure 11), probably the distribution of nanoparticles shows a density gradient along the radial direction of star-like polymer matrix,[17] which is similar to the situations for the distribution of solvent molecules around star polymers in their solution and the distribution of a linear polymer chain around star polymers in the mixture of star and linear polymers.[35,36] The concentration of nanoparticles is zero in the center of star-like polymers and the highest in the region of chain ends.

From the computational simulation results in the previous reports,[37−39] there are three possible stable states of nanoparticle organization in star polymer melts: (a) direct contact, (b) bridging structure, and (c) two polymer layers between nanoparticles. From the calculated result, the increase of molecular weight of the stars can quantitatively promote the state of the bridging structure and suppress the state of direct contact.[37] So we speculate that in the unentangled SPS, the state of POSS nanoparticles is dominated by direct contact between POSS nanoparticles. On the other hand, when the arm of SPS is short ($M_a < M_c$), no entanglements between polymer chains are formed, and the area where the arm ends of SPS

dx.doi.org/10.1021/jp502946d | J. Phys. Chem. B 2014, 118, 5229−5239

congregate is small (Figure 12), thus the contacting area between SPS and POSS nanoparticles is also small.[36] Although

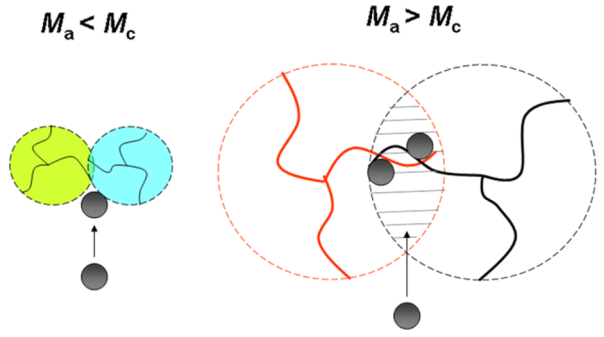

Figure 12. Schematic diagram for the effect of M_a (arm molecular weight) on possible contacting states of star polymers and the distribution state of nanoparticles.

there is attractive interaction (dispersion force) between POSS nanoparticles and SPS chain ends, the contacting area between SPS and POSS nanoparticles is small and the number of interaction sites is low, which results in weak interaction between SPS and POSS nanoparticles. When shear is applied to the SPS/POSS system with the low content of POSS, POSS acts as lubricators between SPS macromolecules in the melt during shear flow. This will result in the reduction of melt viscosity of SPS/POSS composites compared to that of pure SPS. However, if there is strong interaction between star polymer (such as SPS) and nanoparticles, the nanoparticles will act as physical cross-linking sites, so melt viscosity of SPS/nanoparticle system might be higher than (or the same as) that of pure SPS. Very recently Kumar' group has shown that the increasing interaction between polymer chains and nanoparticles promotes the trend of increased viscosities of polymer nanocomposites compared to the those of the pure polymers.[34]

When the arm of SPS is longer ($M_a > M_c$), the melt viscosity of SPS mainly depends on the entanglement number of the arm chains. Only the free end part of the arm chains in the SPS can join the formation of the entanglement site (the other end on the one arm chain was fixed by other arm chains, Figure 12). The presence of nanoparticles will disturb the entanglements of macromolecular chains near the nanoparticles, which may reduce the chain entanglement to some extent.[28] However, in the case of star polymers, the nanoparticles are mainly distributed in the region where the chain ends are located. Owing to weak chain entanglements in the region of chain ends, the presence of nanoparticles only reduces the entanglement number of arm chains slightly, which leads to the reduction of melt viscosity somewhat. On the other hand, the area where the arm ends of SPS congregate becomes large as the arm length of SPS increases, especially when the arm chains start to entangle, and accordingly, the contacting area between SPS and nanoparticles should be large. Furthermore, for the entangled SPS matrix, according to the computational simulation results,[37] the dominated state of POSS nanoparticles is a bridging structure. This means that POSS nanoparticles can contact with more arm chains from different SPS macromolecules. As there is attractive interaction (dispersion force) between POSS nanoparticles and SPS chain ends, which will block chain disentanglements to some extent, and the relaxation time increases, the melt viscosity increases compared to the melt viscosities of the star polymers. The balance between the above two effects [(1) block chain disentanglements due to attractive interaction between polymer chains and nanoparticles; (2) reduce chain entanglements due to the presence of nanoparticles)] dominates the final changing trends of melt viscosity of polymer nanocomposites.

On the basis of the above discussion, we further analyze the dependence of complex viscosity at the terminal frequency region on the arm molecular weight (M_a) and arm number of star PS after adding 1 wt % POSS. Table 4 lists the comparing results. Very interestingly, the change percentage of the complex viscosity at 0.05 rad/s showed the dependence on the arm molecular weight (M_a) and arm number of star PS. In the case of star PS with $M_a < M_c$ ($M_c \approx 32$k for PS), when the arm number remains constant (here three arms), the change percentage reduces with the increase of M_a (S3PS-48k system vs S3PS-75k system); when the M_a remains constant, the change percentage increases with the increase of arm number (S3PS-48k system vs S6PS-93k system). These results are consistent with the above analysis. When the arm of SPS is short ($M_a < M_c$), no entanglements between polymer chains are formed, and the area where the arm ends of SPS congregate is small, especially in the SPS with the high arm number and low arm molecular weight. In this case, nanoparticles are almost located in the outside region surrounding SPS. Thus, the

Table 4. Dependence of Complex Viscosity on the Arm Molecular Weight (M_a) and Arm Number of Star PS after Adding 1 wt % POSS

sample	M_a (kg/mol)	arm no.	POSS (wt %)	$10^{-3}\eta^*_{0.05}$ (Pa·s)[a]	change percentage (%)[b]
S3PS-48k-0	16	3	0	25.8	–
S3PS-48k-1-POSS	16	3	1	10.2	−60.5
S3PS-75k	25	3	0	55.1	–
S3PS-75k-1-POSS	25	3	1	37.9	−31.2
S6PS-93k	15.5	6	0	33.4	–
S6PS-93k-1-POSS	15.5	6	1	10.6	−68.3
S3PS-119k-0	39.7	3	0	120.2	–
S3PS-119k-1-POSS	39.7	3	1	124.6	3.7
S3PS-150k	50	3	0	140.5	–
S3PS-150k-1-POSS	50	3	1	240.7	71.3
S6PS-226k	37.7	6	0	176.6	–
S6PS-226k-1-POSS	37.7	6	1	183.2	3.7

[a]The complex viscosity ($\eta^*_{0.05}$) was obtained at 0.05 rad/s. [b]Calculated by ($\eta^*_{0.05}$ of PS composites with 1 wt % POSS − $\eta^*_{0.05}$ of parental pure PS)/$\eta^*_{0.05}$ of parental pure PS. A dash indicates the reduction percentage.

dx.doi.org/10.1021/jp502946d | J. Phys. Chem. B 2014, 118, 5229−5239

contacting area between SPS and POSS nanoparticles is very small; as a result, the number of interaction sites is very low. When shear is applied to the SPS/POSS system with the low content of POSS, POSS more easily acts as lubricators in between SPS macromolecules in the melt during shear flow.

In contrast, in the case of star PS with $M_a > M_c$, when the arm number remains constant (here three arms), the change percentage increases with the increase of M_a (S3PS-119k system vs S3PS-150k system), which results from strong interaction between SPS and POSS due to large contacting area between two components. When the M_a is very close, the change percentage is almost the same with the increase of arm number (S3PS-119k system vs S6PS-226k system). This is probably ascribed to the approaching M_c of the M_a. This case is a critical region where the behavior is reversed. However, if the M_c is much higher than the M_a, we think that the change percentage will decrease with the increase of the arm number, as the increase of the arm number in star polymers will result in the difficulty in the interdiffusion between the arm chains from the contacting star polymers, so the area where the arm ends of SPS congregate becomes small. As a result, the contacting area between SPS and POSS nanoparticles (or the number of interaction sites) is very small. In this case, the increment of melt viscosity after adding 1 wt % POSS will become small too.

CONCLUSION

The influence of incorporated POSS on the rheological properties of SPS polymer matrix strongly depended on the molecular weight of the arm (M_a) in the SPS, which is similar to the observed phenomenon in SPS/C_{60} system. When the M_a of SPS was smaller than the M_c of PS, the η_0 of SPS composites with a low amount of POSS was lower than that of pure SPS. When the M_a of SPS was higher than the M_c of PS, the η_0 of SPS composites with a low amount of POSS was higher than that of pure SPS. The results from the nonlinear viscosity of the system were in coincidence with the linear rheological results. Furthermore, the Cox−Merz empirical relationship was verified to be valid for SPS and its composites with 1 wt % POSS. The time−temperature superposition (TTS) principle was applied in S3PS-75k, S3PS-150k, and their composites with POSS. Compared to the case of pure SPS, the addition of nanoparticles in the SPS matrix changed the relaxation time, free volume at the reference temperature. The changing trend of viscosity was in accordance with that of relaxation time. We speculated that the incorporation of POSS changed the relaxation mode of the polymer chain that made the viscosity changing with the concentration of POSS. Further investigations, especially theoretical and simulation works, are needed to thoroughly understand the mechanism behind the melt viscosity behavior of star polymer/nanoparticle composites. In addition, we think that the observed phenomenon might be common in other nonlinear polymer/nanoparticle systems, such as H-type or comb-like polymer systems. This will be our next goal in the continuous research.

ASSOCIATED CONTENT

Supporting Information

Table S1 and Figures S1−S8 giving additional rheological data (cross frequencey, relaxation time, plateau modulus, viscosity, glass transition temperature; storage and loss moduli and complex viscosity vs angular frequency; shear viscosity vs shear rate; dynamic and steady state viscosities) and TEM images of S3PS/POSS composites (Figure S9) mentioned in the main text. This material is available free of charge via the Internet at http://pubs.acs.org.

AUTHOR INFORMATION

Corresponding Author

*T. Tang: tel, +86 (0) 431 85262004; fax, +86 (0) 431 85262827; e-mail. ttang@ciac.ac.cn.

Notes

The authors declare no competing financial interest.

ACKNOWLEDGMENTS

This work is financially supported by the National Natural Science Foundation of China for the Projects (51233005, 51073149, and 20804045).

REFERENCES

(1) Li, G.; Pittman, C. U. Polyhedral Oligomeric Silsesquioxane (POSS) Polymers, Copolymers, and Resin Nanocomposites, In *Macromolecules Containing Metal and Metal-Like Elements*; John Wiley & Sons, Inc.: New York, 2005; pp 79−131.

(2) Kuo, S.-W.; Chang, F.-C. POSS Related Polymer Nanocomposites. *Prog. Polym. Sci.* **2011**, *36*, 1649−1696.

(3) Mantz, R. A.; Jones, P. F.; Chaffee, K. P.; Lichtenhan, J. D.; Gilman, J. W.; Ismail, I. M. K.; Burmeister, M. J. Thermolysis of Polyhedral Oligomeric Silsesquioxane (POSS) Macromers and POSS−Siloxane Copolymers. *Chem. Mater.* **1996**, *8*, 1250−1259.

(4) Madbouly, S. A.; Otaigbe, J. U.; Nanda, A. K.; Wicks, D. A. Rheological Behavior of POSS/Polyurethane−Urea Nanocomposite Films Prepared by Homogeneous Solution Polymerization in Aqueous Dispersions. *Macromolecules* **2007**, *40*, 4982−4991.

(5) Fina, A.; Tabuani, D.; Peijs, T.; Camino, G. POSS Grafting on PPgMA by One-step Reactive Blending. *Polymer* **2009**, *50*, 218−226.

(6) Fina, A.; Tabuani, D.; Frache, A.; Camino, G. Polypropylene−polyhedral Oligomeric Silsesquioxanes (POSS) Nanocomposites. *Polymer* **2005**, *46*, 7855−7866.

(7) Zhao, Y. Q.; Schiraldi, D. A. Thermal and Mechanical Properties of Polyhedral Oligomeric Silsesquioxane (POSS)/Polycarbonate Composites. *Polymer* **2005**, *46*, 11640−11647.

(8) Joshi, M.; Butola, B. S.; Simon, G.; Kukaleva, N. Rheological and Viscoelastic Behavior of HDPE/Octamethyl-POSS Nanocomposites. *Macromolecules* **2006**, *39*, 1839−1849.

(9) Jones, P. J.; Cook, R. D.; McWright, C. N.; Nalty, R. J.; Choudhary, V.; Morgan, S. E. Polyhedral Oligomeric Silsesquioxane−polyphenylsulfone Nanocomposites: Investigation of the Melt-flow Enhancement, Thermal Behavior, and Mechanical Properties. *J. Appl. Polym. Sci.* **2011**, *121*, 2945−2956.

(10) Li, G.; Wang, L.; Ni, H.; Pittman, C., Jr. Polyhedral Oligomeric Silsesquioxane (POSS) Polymers and Copolymers: A Review. *J. Inorg. Organomet. Polym.* **2001**, *11*, 123−154.

(11) Markovic, E.; Constantopolous, K.; Matisons, J. In *Applications of Polyhedral Oligomeric Silsesquioxanes*; Hartmann-Thompson, C., Ed.; Springer: Netherlands, 2011; Vol. 3, pp 1−46.

(12) Glodek, T. E.; Boyd, S. E.; McAninch, I. M.; LaScala, J. J. Properties and Performance of Fire Resistant Eco-composites Using Polyhedral Oligomeric Silsesquioxane (POSS) Fire Retardants. *Compos. Sci. Technol.* **2008**, *68*, 2994−3001.

(13) Wu, J.; Haddad, T. S.; Kim, G.-M.; Mather, P. T. Rheological Behavior of Entangled Polystyrene−Polyhedral Oligosilsesquioxane (POSS) Copolymers. *Macromolecules* **2007**, *40*, 544−554.

(14) Kopesky, E. T.; Haddad, T. S.; Cohen, R. E.; McKinley, G. H. Rheological Behavior of Entangled Polystyrene−Polyhedral Oligosilsesquioxane (POSS) Copolymers. *Macromolecules* **2004**, *37*, 8992−9004.

(15) Romero-Guzmán, M.; Romo-Uribe, A.; Zárate-Hernández, B. M.; Cruz-Silva, R. Viscoelastic Properties of POSS−styrene Nanocomposite Blended with Polystyrene. *Rheol. Acta* **2009**, *48*, 641−652.

(16) Fu, B. X.; Gelfer, M. Y.; Hsiao, B. S.; Phillips, S.; Viers, B.; Blanski, R.; Ruth, P. Physical Gelation in Ethylene−propylene Copolymer Melts Induced by Polyhedral Oligomeric Silsesquioxane (POSS) Molecules. *Polymer* **2003**, *44*, 1499−1506.
(17) Tan, H.; Xu, D.; Wan, D.; Wang, Y.; Wang, L.; Zheng, J.; Liu, F.; Ma, L.; Tang, T. Melt Viscosity Behavior of C_{60} Containing Star Polystyrene Composites. *Soft Matter* **2013**, *9*, 6282−6290.
(18) Tuteja, A.; Mackay, M. E.; Hawker, C. J.; Van Horn, B. Effect of Ideal, Organic Nanoparticles on the Flow Properties of Linear Polymers: Non-Einstein-like Behavior. *Macromolecules* **2005**, *38*, 8000−8011.
(19) Rubinstein, M.; Colby, R. H. *Polymer Physics*; Oxford University Press: New York, 2003; pp 309−422.
(20) Liu, C.; He, J.; Ruymbeke, E. v.; Keunings, R.; Bailly, C. Evaluation of Different Methods for the Determination of the Plateau Modulus and the Entanglement Molecular Weight. *Polymer* **2006**, *47*, 4461−4479.
(21) Kim, D.; Srivastava, S.; Narayanan, S.; Archer, L. A. Polymer Nanocomposites: Polymer and Particle Dynamics. *Soft Matter* **2012**, *8*, 10813−10818.
(22) Ferry, J. D. *Viscoelastic Properties of Polymers*, 3rd ed.; J.Wiley & Sons: New York. 1980.
(23) Williams, M. L.; Landel, R. F.; Ferry, J. D. The Temperature Dependence of Relaxation Mechanisms in Amorphous Polymers and Other Glass-forming Liquids. *J. Am. Chem. Soc.* **1955**, *77*, 3701−3707.
(24) Cox, W. P.; Merz, E. H. Correlation of Dynamic and Steady Flow Viscosities. *J. Polym. Sci.* **1958**, *28*, 619−622.
(25) Milner, S. T. Relating the Shear-thinning Curve to the Molecular Weight Distribution in Linear Polymer Melts. *J. Rheol.* **1996**, *40*, 303−315.
(26) Doi, M.; Edwards, S. F. Dynamics of Concentrated Polymer Systems. Part 2.-Molecular Motion Under Flow. *J. Chem. Soc., Faraday Trans. 2: Mol.Chem. Phys.* **1978**, *74*, 1802−1817.
(27) Tuteja, A.; Duxbury, P. M.; Mackay, M. E. Multifunctional Nanocomposites with Reduced Viscosity. *Macromolecules* **2007**, *40*, 9427−9434.
(28) Gordon, G. V.; Schmidt, R. G.; Quintero, M.; Benton, N. J.; Cosgrove, T.; Krukonis, V. J.; Williams, K.; Wetmore, P. M. Impact of Polymer Molecular Weight on the Dynamics of Poly-(dimethylsiloxane)-Polysilicate Nanocomposites. *Macromolecules* **2010**, *43*, 10132−10142.
(29) Schmidt, R. G.; Gordon, G. V.; Dreiss, C. c. A.; Cosgrove, T.; Krukonis, V. J.; Williams, K.; Wetmore, P. M. A Critical Size Ratio for Viscosity Reduction in Poly(dimethylsiloxane)-Polysilicate Nanocomposites. *Macromolecules* **2010**, *43*, 10143−10151.
(30) Jain, S.; Goossens, J. G. P.; Peters, G. W. M.; van Duin, M.; Lemstra, P. J. Strong Decrease in Viscosity of Nanoparticle-filled Polymer Melts Through Selective Adsorption. *Soft Matter* **2008**, *4*, 1848−1854.
(31) Nagarajan, R.; Barry, M.; Ruckenstein, E. Unusual Selectivity in Solubilization by Block Copolymer Micelles. *Langmuir* **1986**, *2*, 210−215.
(32) Mountrichas, G.; Pispas, S.; Xenogiannopoulou, E.; Aloukos, P.; Couris, S. Aqueous Dispersions of C_{60} Fullerene by Use of Amphiphilic Block Copolymers: Preparation and Nonlinear Optical Properties. *J. Phys. Chem. B* **2007**, *111*, 4315−4319.
(33) Dintcheva, N. T.; Morici, E.; Arrigo, R.; La Mantia, F. P.; Malatesta, V.; Schwab, J. J. Structure-properties Relationships of Polyhedral Oligomeric Silsesquioxane (POSS) Filled PS Nanocomposites. *Express Polym. Lett.* **2012**, *6*, 561−571.
(34) Kalathi, J. T.; Grest, G. S.; Kumar, S. K. Universal Viscosity Behavior of Polymer Nanocomposites. *Phys. Rev. Lett.* **2012**, *109*, 198301.
(35) Huissmann, S.; Blaak, R.; Likos, C. N. Star Polymers in Solvents of Varying Quality. *Macromolecules* **2009**, *42*, 2806−2816.
(36) Truzzolillo, D.; Vlassopoulos, D.; Gauthier, M. Osmotic Interactions, Rheology, and Arrested Phase Separation of Star-Linear Polymer Mixtures. *Macromolecules* **2011**, *44*, 5043−5052.
(37) Zhao, L.; Li, Y. G.; Zhong, C. Integral Equation Theory Study on The Structure and Effective Interactions in Star Polymer Nanocomposite Melts. *J. Chem. Phys.* **2007**, *126*, 014906.
(38) Hooper, J. B.; Schweizer, K. S. Contact Aggregation, Bridging, and Steric Stabilization in Dense Polymer-Particle Mixtures. *Macromolecules* **2005**, *38*, 8858−8869.
(39) Hooper, J. B.; Schweizer, K. S. Theory of Phase Separation in Polymer Nanocomposites. *Macromolecules* **2006**, *39*, 5133−5142.